A Technical and Economic Assessment of Transport and Storage of CO_2 in Deep Saline Aquifers for Power Plant Greenhouse Gas Control

Sean McCoy
Department of Engineering and Public Policy
Carnegie Mellon University
Pittsburgh, PA. 15213

Abstract

Global efforts to reduce greenhouse gas emissions have stimulated considerable interest in carbon capture and sequestration (CCS) as a potential "bridging technology" that can achieve significant CO_2 emission reductions while allowing fossil fuels to be used until alternative energy sources are more widely deployed. Electric power plants are among the most attractive sources for CCS since they are point sources that are responsible for nearly 39% of all anthropogenic CO_2 emissions in the United States. From an engineering standpoint, the most promising sinks for the storage of captured CO_2 appear to be geological formations. Options for the storage of CO_2 include: producing and depleted oil reservoirs, deep unminable coal seams and, deep saline aquifers. This paper presents engineering and economic models of transport of CO_2 by pipeline to the storage site and geological storage in deep saline aquifers. A case study considering storage of CO_2 from a 500 MW pulverized coal (PC) power plant in the Wabamun Lake area of Alberta, Canada has shown that the median cost of transport and storage is $1.94 per tonne of CO_2 stored ranging from a 5^{th} percentile of $0.78 per tonne to a 95^{th} percentile $14.59 per tonne. The variability of the transport and storage cost is found to be primarily due to the reservoir parameters, transport distance, and plant capacity factor. Based on these results, the cost of transport and storage is a small part of the total cost of CCS, but there will be cases in which the cost of transport and storage are large. The strong dependence of the transport and storage cost on the reservoir parameters implies that cost estimates for transport and storage must take this variability into account, and that policies aimed at encouraging reductions in CO_2 emissions in the power sector via CCS must recognize that this option may not be economically viable in all cases.

Advisor: Edward S. Rubin
Word Counts: 5427 (main text); 7733 (total paper)
Page Count: 24 (main text); 35 (total paper)

1. Introduction

Large reductions in carbon dioxide emissions from energy production will be required in the near future to stabilize atmospheric concentrations of CO_2[1,2]. One option to reduce carbon intensity while allowing for continued use (in the short-term) of fossil fuels is carbon capture and storage (CCS); i.e., the capture of CO_2 directly from anthropogenic sources and disposal of it in geological sinks for significant periods of time[3]. CCS requires CO_2 to be captured from energy production processes, compressed to high pressures, transported to a storage site, and injected into a suitable geologic formation. Each of these steps is capital and energy intensive, and will have a significant impact on the cost of energy production. Government regulators, policy-makers (public and private), and other interested parties require methods to estimate the cost of geological carbon storage. While many studies of carbon capture processes have been undertaken[4-6] and reasonable engineering-economic models have been developed[7], there is a paucity of engineering-economic models for transport and storage.

This paper details the development of models to determine the cost of CO_2 transport from the site of capture to the location of storage via pipeline, and the cost of subsequent storage in a deep saline aquifer[*]. Both models will be discussed in the context of the electric power industry, which generates nearly 39% of all CO_2 emissions in the United States from large point sources[8]. In this context, the cost per tonne of transporting and storing CO_2 from a range of capacities of power plants will be determined and, the effect of varying pipeline design parameters and geological parameters will be quantified. Furthermore, in an attempt to quantify sensitivity of the models to uncertainty and variability in design parameters, a probabilistic analysis will be performed, which shows the range of costs that could occur and the probability associated with these costs.

2. Background

2.1. Alternative Options for Transport

There are multiple options for transporting compressed CO_2 from the site of capture to the site of storage. Practical modes of overland transport include motor carrier, rail, and pipeline. The most economic method of transport depends on the locations of capture and storage, distance from source to sink, and the quantities of CO_2 to be transported. However, the quantity to be transported is the dominant factor- on the order of 5 million metric tonnes (Mt) per year of CO_2 would need to be transported from a single 500 MW coal-fired power plant. Assuming that either a motor carrier or rail car could move approximately 50 tonnes (t) of CO_2 per trip, there would be a need for over 200 tanker trips or rail cars per day, making both these options logistically challenging and expensive. This leaves pipeline as the only viable option for overland transport[9,10].

[*] A formation lying at least 800m below the ground surface whose fluid saturation, porosity and permeability allows the production of saline water. The water produced from formations at these depths is unfit for industrial or agricultural use, or human consumption.

2.2. Alternative Options for Geological Storage

Geological sinks for storing captured CO_2 include: mined salt caverns, producing oil reservoirs, deep unminable coal beds, depleted hydrocarbon reservoirs, and deep saline aquifers. Storage of CO_2 in producing oil reservoirs and coal beds are referred to as enhanced oil recovery (EOR) and enhanced coal bed methane (ECBM) recovery. Selecting one storage option over another in a specific case would depend on assessments of the geological suitability of the sedimentary basin[†], the inventory of potential storage sites, the safety and long term fate of injected CO_2, and the capacity of the storage sites[11]. Table 1 shows the range of capacity estimates for deep saline aquifers, EOR, and ECBM reported by different authors[12-19].

Table 1. Range of CO_2 storage capacity estimates for deep saline aquifers, EOR, and ECBM reported by several authors[12-19].

Formation	United States (Gt CO_2)	Worldwide (Gt CO_2)
Deep Saline Aquifers	10^2	10^2-10^4
EOR & Depleted Oil and Gas Fields	10^2	10^2-10^3
ECBM	10^1	10^2

On a global scale, the estimated capacity of deep saline aquifers is largest, followed by oil and gas reservoirs (including depleted reservoirs) and ECBM, while mined salt caverns have an estimated global storage capacity that is insignificant in comparison. However, a recent regional scale estimate for the capacity of deep saline aquifers not included in the above table has made an estimate on the order of 10^3 Gt CO_2 for the Alberta basin alone[20] using a method of estimation that accounts for solubility trapping. Thus, deep saline aquifers show the strongest potential for geological storage of anthropogenic CO_2 in the long-term because of large storage capacities.

3. Pipeline Transport of Carbon Dioxide

3.1. Industrial Experience

There is considerable industrial experience in the transport of CO_2 by pipeline. Upwards of 50 Mt/y of CO_2 is transported over nearly 3100 km of pipelines primarily for use in EOR operations[21-24]. For comparison, this would be the amount of CO_2 produced by ten-500 MW coal fired power plants.

3.2. Special Considerations

Efficient transport of CO_2 via pipeline can be accomplished by compressing and cooling the CO_2 to the supercritical fluid state. Transportation at lower densities is inefficient because of the large volumes that need to be moved. The supercritical fluid state for CO_2

[†] A sedimentary basin is a depression in the earth's crust formed by movement of tectonic plates where sediments have accumulated to form sedimentary rocks. Hydrocarbons commonly occur in sedimentary basins.

occurs at conditions greater than the supercritical pressure and temperature- 7.38 MPa and approximately 31°C- as shown in the phase diagram in Figure 1. Transport of CO_2 at pressures above supercritical ensures that potentially damaging mixtures of gas and liquid (i.e. two-phase flow) in the pipeline do not occur.

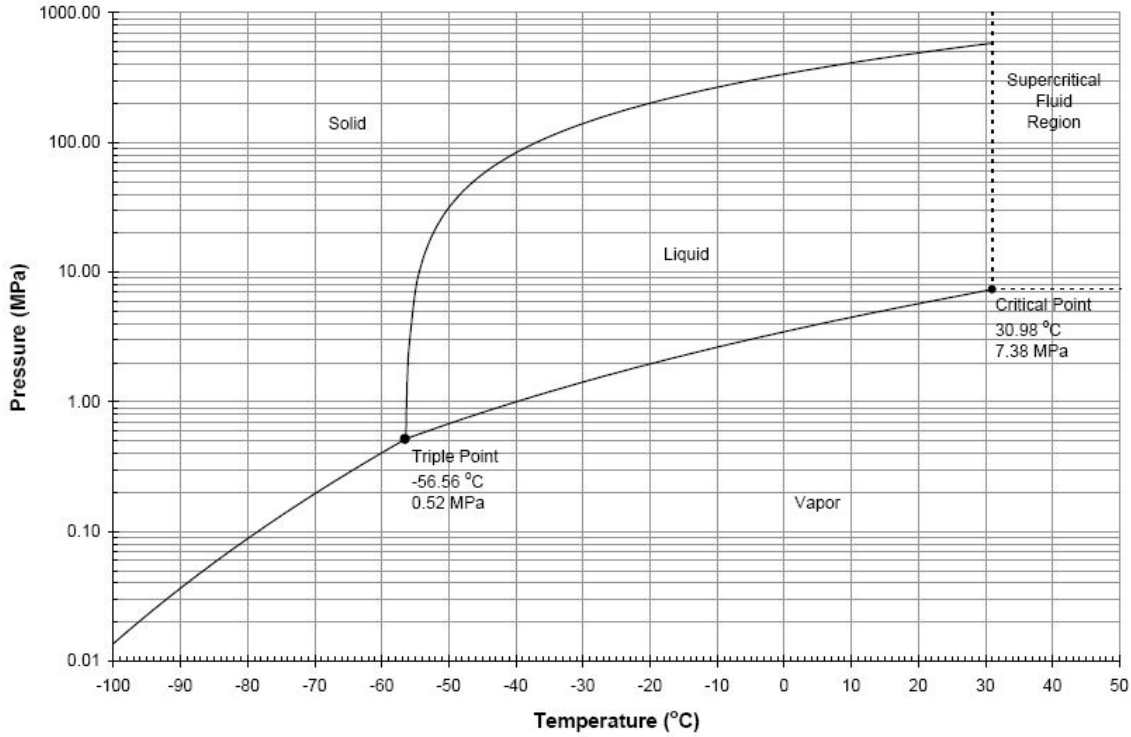

Figure 1. Phase diagram for CO_2 showing the sublimation, melting, and boiling curves as well as the triple point and the critical point

To ensure that the flow in the pipeline remains single phase, i.e. at pressures greater than 7.38 MPa, pipeline operators recommend that the CO_2 pressure not be allowed to drop below 10.3 MPa at the outlet of the pipeline[23].

Unfortunately, handling of supercritical CO_2 presents some difficulties. Traditional gaskets loose their elastic properties and hydrocarbon lubricants become infective when subjected to supercritical CO_2[22]. In addition, CO_2 in the presence of moisture can produce carbonic acid, which can easily corrode carbon steel used in oil and natural gas pipelines [22,25]. Thus, the CO_2 should be relatively dry before transport, and appropriate design measures must be taken to ensure that the pipeline and compressor materials are suited to handling supercritical CO_2.

3.3. Model Development

The transport model developed in this research takes engineering and design parameters, such as pipeline length and design CO_2 mass flow, as well as economic parameters, such as the fixed charge factor, and operating and maintenance charges as input. From these inputs the required pipe diameter and cost per tonne of CO_2 transported are calculated.

The transport model is based on previous work by the Massachusetts Institute of Technology (MIT) for the United States Department of Energy (DOE)[23] and has been extended to include a comprehensive physical properties model for CO_2, booster pumping station options, segment elevation changes, and probabilistic assessment capabilities. The boundaries, and primary inputs and outputs of the transport model are summarized in Figure 2.

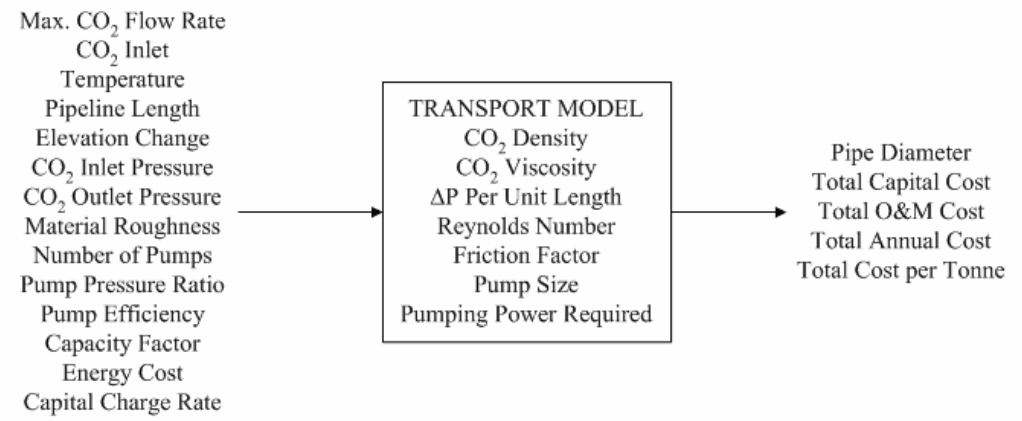

Figure 2. The boundaries, inputs, and output of the pipeline model.

The pipeline model described in the following sections has been implemented in Excel using Visual Basic. A screen capture of the basic input and output screen and details of the solution procedure can be found in Appendix B.

3.3.1. Pipeline Engineering and Design

The pipeline is modeled as a series of pipe segments located between booster pumping stations. From the input information to the transport model, the required pipeline diameter for each segment is calculated. Based on this pipeline segment diameter and length, the cost of the segment is calculated.

The pipeline segment diameter, D, is calculated from a mechanical energy balance on the flowing CO_2, which can be found in Appendix B. In the simplification of the energy balance, supercritical CO_2 is considered an incompressible fluid[‡] and the pipeline flow and pumping processes are treated as isothermal. While supercritical CO_2 is not actually incompressible, this assumption greatly simplifies the energy balance. These simplifications result in Equation 1:

$$D = \left[\frac{32 f_F \Delta L \dot{m}^2}{\pi^2 \Delta p \rho + g \pi^2 \rho^2 \Delta Z} \right]^{1/5} \quad (1)$$

[‡] Incompressible fluids, such as water, maintain a nearly constant density as a function of pressure. Hence, incompressible fluids are "pumped", rather than compressed like a gas.

where f_F is the Fanning friction factor, ΔL is the pipeline segment length, $\dot{m}$ is the design (i.e. maximum annual) mass flow rate of CO_2, Δp is the pressure drop over the pipe segment, g is acceleration due to gravity, ΔZ is the elevation change over the pipeline segment, and ρ is the density of the flowing CO_2. Thus, Equation 1 can be used to calculate the pipe diameter required for a given pressure drop[§]. Complicating this, however, is the Fanning friction factor, which is a function of the pipe diameter. The Fanning friction factor can not be solved for analytically, thus an explicit approximation for Fanning friction factor is given by Equation 2[26].

$$\frac{1}{2\sqrt{f_F}} = -2.0\log\left\{\frac{\varepsilon/D}{3.7} - \frac{5.02}{\mathrm{Re}}\log\left[\frac{\varepsilon/D}{3.7} - \frac{5.02}{\mathrm{Re}}\log\left(\frac{\varepsilon/D}{3.7} + \frac{13}{\mathrm{Re}}\right)\right]\right\} \qquad (2)$$

where ε is the roughness of the pipe, and Re is the Reynolds number. The Reynolds number is given by Equation 3:

$$\mathrm{Re} = \frac{4\dot{m}}{\mu\pi D} \qquad (3)$$

where μ is the viscosity of the fluid. As a result, Equations 1, 2, and 3 must be solved iteratively to determine the pipe diameter. Further details of the solution method can be found in Appendix B.

3.3.2. Pumping Station Engineering and Design

Booster pumping stations may be required for longer pipeline distances or for pipelines in mountainous or hilly regions. Additionally, the use of booster pumping stations may allow a smaller pipe diameter to be used, reducing the cost of CO_2 transport. The pumping station size is developed from the energy balance on the flowing CO_2 (see Appendix B) in a manner similar to the calculation of the pipe segment diameter.

Both the pumping station size and pipeline diameter are calculated on the basis of the design mass flow rate of CO_2, while the pumping station annual power consumption is calculated on the basis of the nominal mass flow rate of CO_2[**]. Pumping station size is required to determine the capital cost of the pump, while the pumping station annual power requirement is required to calculate the operating cost due to energy consumption.

[§] This equation is valid for flow of any incompressible fluid, such as a dilute mixture of CO_2 and hydrogen sulfide (H_2S) or sulfur dioxide (SO_2). However, the model assumes that the fluid is pure CO_2.

[**] The nominal mass flow rate of CO_2 is the product of the power plant capacity factor and the design mass flow rate of CO_2.

3.3.3. Pipeline Economics

The data for the pipeline economics are primarily from a model developed for the United States Department of Energy (DOE) by the Massachusetts Institute of Technology (MIT)[23]. The capital cost of the CO_2 pipeline is based on capital cost data for natural gas pipelines contained in the United States' Federal Energy Regulatory Commission (FERC) filings and published in the Oil and Gas Journal[23]. From the FERC information, the total cost of construction of the pipeline, including materials, right-of-way, labor, and miscellaneous components (e.g. surveying, engineering, administration, etc.) is $828,161 per meter of pipe diameter per kilometer of pipeline length. The operating and maintenance (O&M) charges were reported to be approximately $3,100 per kilometer of pipeline for current pipelines.

The total capital cost (TCC) of a pumping station has been estimated by the IEA for a study involving the pipeline transmission of CO_2[25]. That cost is given by Equation 4:

$$TCC = 7.82P + 0.46 \quad (4)$$

where *TCC* is in millions of US dollars, and *P* is the installed booster station power in MW. This correlation yields a cost slope of $7,820 per kW of installed capacity.

The annual cost of the pipeline is calculated in 1999 dollars by annualizing the total capital cost over the life of the pipeline at the given discount rate, and adding the annual pipeline O&M cost, the annual pump O&M cost, and the cost of energy for the booster stations. The TCC is given by Equation 5, and the total annual O&M cost by Equation 6:

$$TCC = 828160.59\left[D_1 + D_n\left(N_S - 1\right)\right]L + 10^6\left(7.82P + 0.46\right)N_B \quad (5)$$

$$O\,\&\,M = 3100L + C_P P N_B \quad (6)$$

where: L is the total pipeline length; D_1 is the initial segment diameter; D_n is the n^{th} segment diameter; N_S is the number of pipe segments; N_B is the number of booster compressors, and; C_p is the cost of power.

4. Storage of Carbon Dioxide in Deep Saline Aquifers

4.1. Storage Projects and Industrial Analogues

There is one industrial scale CCS project currently in operation in the North Sea, while processes analogous to those used in deep saline aquifer storage are used for acid gas[††]

[††] Formally, an acid gas is any gas that can form acidic solutions when mixed with water. In this context, an acid gas is a mixture of hydrogen sulfide (H_2S) and CO_2 of varying proportions. Both gases cause corrosion, and H_2S is

disposal in Canada. The Sleipner project, operated by Statoil, has been injecting approximately 1 Mt/y of CO_2 into the Utsira Formation approximately 800 m below the sea bed[27,28]. Since injection began in October of 1996, over 8 Mt of CO_2 have been injected, which is approximately equivalent to two years of emissions from a 500 MW coal fired power plant. The CO_2 is being injected to the Utsira Formation by Statoil because it was determined to be less costly than paying the Norwegian carbon tax of approximately $40 per tonne of CO_2[29].

In Western Canada, over 4.5 Mt of acid gas have been injected into deep saline aquifers and depleted hydrocarbon reservoirs at 48 sites, produced by 42 separate gas plants[30]. Of the total mass injected, approximately 2.5 Mt is CO_2. Injection of acid gas into reservoirs in Western Canada has been driven by regulatory changes that occurred in 1989, which require that gas plants with a sulfur throughput of 1 t/d or greater recover the sulfur as opposed to flaring the hydrogen sulfide (H_2S) recovered from produced natural gas[31]. Both H_2S and CO_2 are disposed of simultaneously because co-capture of the two gases is less expensive than separate capture of H_2S and CO_2.

4.2. Flow and Injection Processes

The amount of CO_2 that can be injected by one well, $\dot{m}_w$, into a given thickness of formation, h, for a given pressure difference between the aquifer, p_a, and the bottom hole injection pressure (BHIP), p_i, is known as the injectivity[32], I, and is given in Equation 7.

$$I = \frac{\dot{m}_w}{h(p_i - p_a)} \qquad (7)$$

Once the CO_2 moves through the perforations at the bottom of the well bore into the formation, the CO_2 displaces the formation water. The mobility ratio describes the velocity of the displacing fluid (CO_2) relative to the velocity of the fluid being displaced (brine), and is given as Equation 8[33]:

$$M = \frac{\mu_w k_{rc}}{\mu_c k_{rw}} \qquad (8)$$

where μ_w and μ_c are the viscosities of water and CO_2, and k_{rw} and k_{rc} are the relative permeability of the formation to water and CO_2. A mobility ratio greater than 1 means that, under an imposed pressure differential, the CO_2 is capable of traveling at a velocity greater than, or equal to, that of the brine.

4.3. Model Development

The model takes engineering and design parameters, such as formation depth, formation permeability, CO_2 mass flow, and economic parameters, such as project lifetime, discount rate, and monitoring and verification costs as input. From these inputs the

extremely poisonous. In the petroleum industry, H_2S and CO_2 gases are obtained after a sweetening process is applied to a sour gas.

number of wells required and the cost per metric ton of CO_2 injected are calculated. The transport model is based on previous work[23] that has been extended to include a comprehensive physical properties model for CO_2, a BHIP model, and probabilistic assessment capabilities. The boundaries, and primary inputs and outputs of the transport model are summarized in Figure 3.

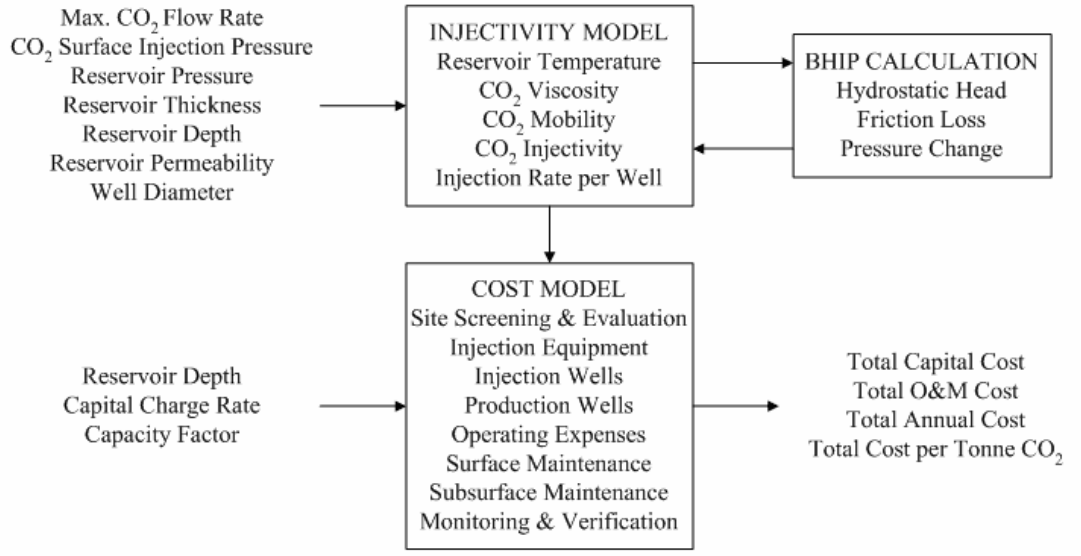

Figure 3. The boundaries, inputs, and output of the deep saline aquifer model.

The pipeline model described in the following sections has been implemented in Excel using Visual Basic. A screen capture of the model input-output screen is shown Appendix B along with details of the model implementation.

4.3.1. Injection Equipment Engineering and Design

Injection equipment can be categorized as surface and sub-surface. The surface equipment category encompasses the distribution piping between the terminus of the CO_2 trunk line and the well heads, CO_2 flow control equipment, and equipment to monitor the well condition[23]. The model does not include compression equipment in the surface equipment category, as in most cases additional compression at the well head will not be required. The sub-surface equipment category includes the injection well (i.e. well casing, and tubing), and the bottom hole pressure monitoring equipment (see Appendix B).

The design and engineering of the surface equipment is not explicit in the model, as the capital and operating costs of the surface equipment are simply a function of the number of injection wells. Thus, the cost of the CO_2 injection into the aquifer is a function of the number of injection wells and the well depth.

The problem of finding the appropriate number of wells for a given geology and injection rate of CO_2 is formulated as a root finding problem. This formulation of

the problem is shown as Equation 9, where $E(N_w)$ is error between the required and calculated flow rate as a function of the number of injection wells, N_w.

$$E(N_w) = \dot{m}_{W,\,req'd}(N_w) - \dot{m}_{W,\,calc}(N_w) \qquad (9)$$

Equation 9 is expanded by substituting the correlation of Law and Bachu[32] for the calculated injection rate, which results in Equation 10.

$$E(N_w) = \frac{\dot{m}}{N_w} - 0.000538\,\frac{\rho(k_h k_v)^{0.5} h(p_i - p_a)}{\mu \ln\left(\frac{r_e}{r_w}\right)} \qquad (10)$$

In Equation 10: $\dot{m}_w$ represents the injection rate; $\dot{m}$ is the total mass injection rate for the project; ρ is the density of CO_2 at formation conditions; h represents the aquifer thickness; p_i is the BHIP; p_a is the far field aquifer pressure; k_h and k_v are the horizontal and vertical permeability of the formation to CO_2; μ is the viscosity of CO_2 under formation conditions; and, r_w and r_e are the radii of the well and injection influence, respectively.

Several important assumptions apply to Equation 10: the aquifer is homogeneous and anisotropic[‡‡]; the injection well is vertical and completed through the full thickness of the aquifer; the properties of CO_2 are constant in the aquifer; and, the radius of influence is constant for the 3 inch diameter well modeled. As a rule of thumb, the logarithm of natural logarithm of the ratio of the radii of injection influence to the well diameter is equal to 7.5[4].

The root of Equation 10 is the appropriate number of wells for a given geology and injection rate of CO_2, and is found using a combination of bracketing and Ridders' Method[§§]. Further details of the solution algorithm can be found in Appendix B.

4.3.2. Storage Economics

The correlations used to determine the capital and operating and maintenance (O&M) costs of the injection equipment are based on the Energy Information Administration cost indices for petroleum production[34] and were developed in a study performed for the DOE[23]. Average equipment costs and O&M costs were determined on a per well basis and, in the case of injection equipment and subsurface maintenance, are scaled by a power of 0.5 to reflect typical economies of scale. The scaling factor accounts for the relationship between the number of

[‡‡] If the actual aquifer is not-homogeneous, and the well is located in a region of the aquifer with higher permeability than average, the injectivity could be much higher than suggested by a calculation using a total average for the aquifer. The opposite also applies: if the well is located in a region of locally lower permeability, the injectivity could be much lower than predicted.

[§§] An algorithm for finding roots which retains that prior estimate for which the function value has opposite sign from the function value at the current best estimate of the root.

wells and the resulting size and complexity of associated surface equipment. Table 2 shows the correlations between the number of wells and costs, where N_w is the number of injection wells and d is the completion depth of the wells in meters. Only an integer-number of wells can be drilled, thus the ceiling of the non-integer number of wells is used for N_w in Table 2. For example, if 3.4 wells are required, the cost is calculated based on 4 wells.

The well drilling cost is calculated based on a correlation developed in the DOE study[23] from data contained in the 1998 Joint Association Survey (JAS) on Drilling Costs report[35]. Regression analysis on drilling cost data for onshore oil and gas wells provided the relationship.

Table 2 Capital and operating and maintenance (O&M) cost correlations for the CO_2 storage model, where N_w is the integer-number of injection wells and D is the completion depth of the wells.

Parameter	Description	Unit	Correlation
Capital Costs			
Injection Equipment	Distribution network piping	\$/well	$43600\left(7389/280N_w\right)^{0.5}$
Drilling Cost		\$/well	$88800e^{0.0008D}$
O&M Costs			
Normal Annual Operating Expenses	Operations employees, etc.	\$/well	6700
Consumables		\$/well	17900
Surface Maintenance	Repairs and services	\$/well	$13600\left(7389/280N_w\right)^{0.5}$
Subsurface Maintenance	Repairs and services	\$/well	$5000d/1219$

The site selection process is also a significant cost item. The cost of preliminary site screening was estimated to be \$330,000 per site and the cost of candidate evaluation was estimated to be \$1,355,000 in a study by Battelle Memorial Institute[22]. The total cost of screening and evaluation is \$1,685,000, which is added to the project capital cost. The cost of monitoring is included in the model as an annual O&M cost on a per tonne stored basis.

The annual cost of the project in 1999 dollars is the sum of the annualized total capital cost, TCC, and the annual O&M costs. The total capital cost and the annual O&M cost are summarized by Equations 11 and 12, respectively.

$$TCC = N_w\left[88800e^{0.008d} + 43600\left(7389/280N_w\right)^{0.5}\right] + 1685000 \qquad (11)$$

$$O\&M = N_w\left[6700 + 17900 + 13600\left(7389/280N_w\right)^{0.5} + 5000d/1219\right] + mC_{monitoring} \qquad (12)$$

5. Case Study

To illustrate the application and utility of the model developed in this research, a case study has been conducted, based on a scenario in which CO_2 is captured from a 500 MW pulverized coal (PC) fired power plant located in the Wabamun Lake area of the province of Alberta, Canada. This region, shown in Figure 4, is host to over 3000 MW of coal fired generation[36] with another 500 MW of generation under construction[37]. The model is used to evaluate the potential cost of injection into a specific candidate formation, identified in Section 5.1.2, from the standpoint of the perspective operator or owner of a power plant[***]. To identify the sensitivity of the outputs to uncertainty and variability in the inputs, a Monte Carlo analysis has been performed on the models.

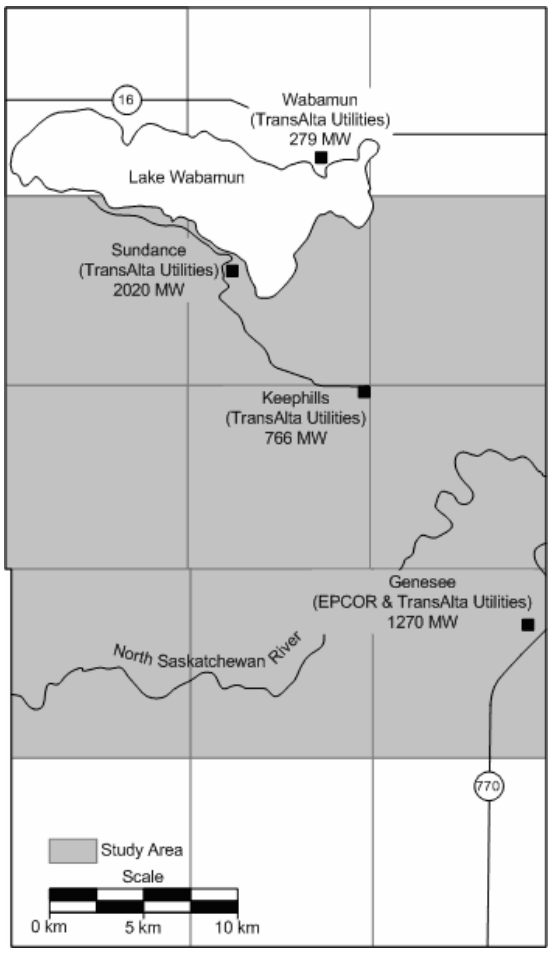

Figure 4. The area surrounding Lake Wabamun in Central Alberta, used as the setting for the case study[36].

[***] i.e., the perspective owner or operator would have control over design aspects of the capture, transport, and storage system, but may not know with certainty the emissions rate of the power plant they will be constructing.

5.1. Case Study Selection

5.1.1. Transport Parameters

The parameters are based on a relatively short pipeline between the CO_2 source and the sink, as the entire Wabamun Lake area sits atop a suitable deep saline aquifer[36,38]. The short pipeline distance and lack of major elevation changes in the region means that booster pumping stations would likely not be required, thus they have been excluded from the analysis. The parameters for this scenario and their distributions are listed in Table 3.

The distribution for annual CO_2 mass flow rate is based on PC plant sizes between 320 MW and 530 MW, or Integrated Gasification Combined Cycle (IGCC) plant sizes between 380 MW and 630 MW[†††] and the distribution for capacity factor is based on data from US Environmental Protection Agency's software package, eGRID2002PC[39]. The distribution for the Annual O&M cost is arbitrary, but covers a reasonable range of operating costs[23], while the Fixed Charge factor distribution is believed to be representative of typical electricity industry rates.

Table 3. The input parameters and their distributions for the transport model

Parameter	Rep. Value	Distribution	a	b	c	μ
CO_2 Mass Flow (Mt/y)	4.67	Uniform	3.00	5.00	-	4.00
Plant Capacity Factor (%)	75	Triangular	15	90	75	60
Inlet Temperature (°C)	5.6	Constant	-	-	-	-
Inlet Pressure (MPa)	13.79	Constant	-	-	-	-
Outlet Pressure (MPa)	10.3	Constant	-	-	-	-
Total Pipeline Length (km)	30	Uniform	10	50	-	30
Pipeline Elevation Change (m)	0	Constant	-	-	-	-
Annual O&M ($/km/y)	3,100	Triangular	2,000	5,000	2,300	3,100
Fixed Charge Factor (%)	1.5	Uniform	10%	20%	-	15%

5.1.2. Storage Parameters

For the Monte Carlo analysis for storage, the distributions listed in Table 4 for the CO_2 mass flow rate, plant capacity factor, and capital recovery factor were used to allow results from the two separate models to be summed to generate a total cost per tonne of CO_2 stored. The monitoring and verification costs for the storage model are based on ranges presented by various authors at recent conferences[40,41], and the site screening and evaluation costs are based on those presented by the Battelle Memorial Institute[22].

[†††] These capacities and annual emissions correspond to emission rates of approximately 1067 kg/MWh for a PC plant and 902 kg/MWh for a IGCC plant.

The formation modeled for storage is a Cretaceous Glauconitic Sandstone aquifer in the Upper Mannville Group[32,36]. This formation is located at depths greater than 1460 m, and overlain by several regional scale aquitards[‡‡‡] that would inhibit upwards movement of the injected CO_2[42]. The variability of the formation permeability has been modeled based on measurements from drillstem tests performed in the course of petroleum exploration in the area[42]. The permeabilities are log-normally distributed with a median (or geometric mean) of 6.28 md[§§§]. The temperature and pressure gradients for the formation are modeled based on studies of the Alberta Basin[42], and sedimentary basins in general[4].

Table 4. The input parameters and their distributions for the storage model

Parameter	Rep. Value	Distribution	a	b	c	μ[****]
Injection Pressure (MPa)	10.3	Constant	-	-	-	-
Depth (m)	1480	Uniform	1460	1620	-	1540
Thickness (m)	14	Triangular	10	20	12	14
Horizontal Permeability (md)	6.28	Truncated Lognormal	1.84	2.00	-	6.28
Pressure Gradient (MPa/km)	8.4	Triangular	8	12	11.5	10.5
Temperature Gradient (°C)	30	Triangular	25	35	30	30
Permeability Anisotropy	0.3	Constant	-	-	-	-
Monitoring & Verification Cost ($/tonne)	0.05	Uniform	0.03	0.10	-	0.07
Site Screening & Evaluation (k$/site)	1,685	Uniform	843	2,528	-	1,685

5.2. Illustrative Case Study Results

Evaluation of the pipeline transport model using the representative parameters listed in Table 3 results in a cost of $0.34 per tonne of CO_2 transported, 92% of which results from capital cost with the remaining 8% accounting for O&M. Figure 5 shows the cost surface that results from varying the pipeline length and plant size for a PC power plant while continuing to assume that no booster stations are required along the pipeline.

Figure 5 shows that the cost of transport increases with distance, and decreases with plant capacity. Moreover, the cost per tonne of CO_2 transported exhibits increasing returns to scale; that is, for a fixed distance the transport cost decreases non-linearly with plant size. For example, for a 200 km pipeline, the cost of transport for a 100 MW power

[‡‡‡] A formation that is saturated with fluid whose porosity and permeability is such that water can not be produced from the formation, in contrast to an aquifer, which can produce water.
[§§§] For the Monte Carlo analysis the permeability is modeled using a truncated lognormal distribution, with a minimum of 0.41 md and a maximum 103.9 md, which correspond to the minimum and maximum permeabilities as measured in the drillstem tests.
[****] In the case of the truncated lognormal distribution, this parameter is the geometric mean of the lognormal distribution or e^{μ}, where μ is the arithmetic mean of ln(X).

plant is $8.96 per tonne, whereas for a 500 MW power plan the cost is approximately $3.17 per tonne, and for a 1000 MW power plant the cost decreases to approximately $2.04 per tonne. The values presented in Figure 9 compare well with those presented by Skovholt[10], which are around of 1€ per tonne (i.e. $1.30 per tonne) of CO_2 transported over 100 km by pipelines for plants ranging between 100MW to 1000 MW.

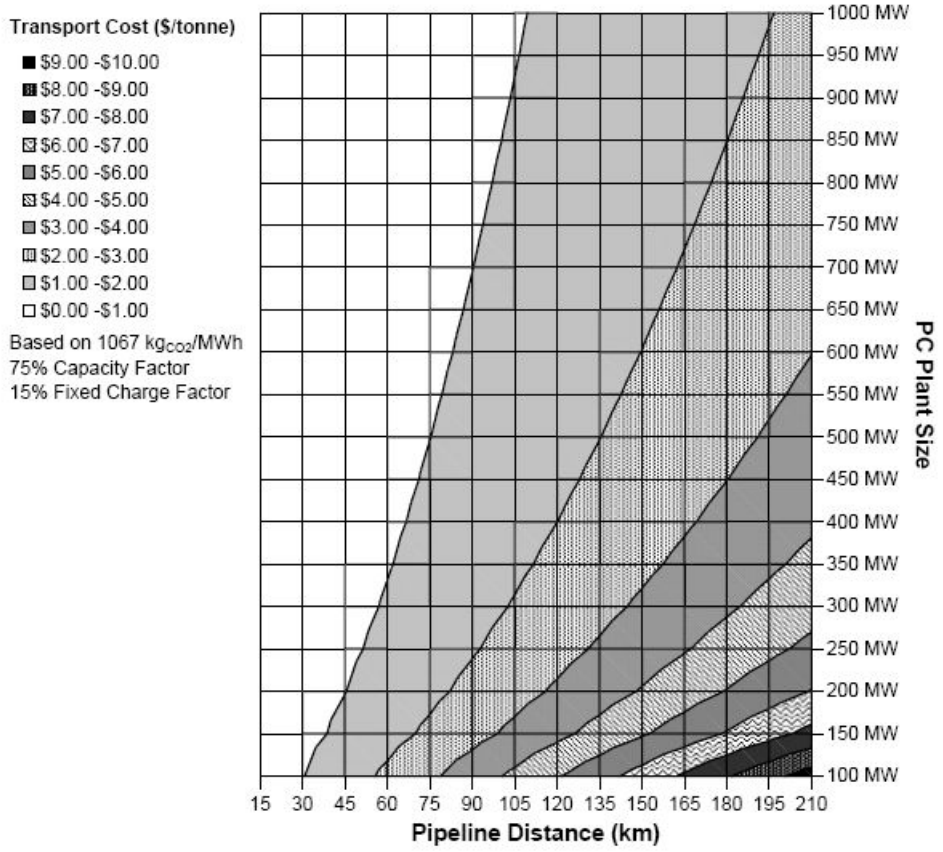

Figure 5. The transport cost surface for a coal fired power plant with no booster stations.

Using the representative parameters listed in Table 4 and the emissions rate for a coal-fired plant, the cost of aquifer storage is $0.80 per tonne of CO_2 stored, injected through 25 wells into the aquifer. The cost of aquifer storage in dollars per tonne for coal-fired plants of varying capacities injecting CO_2 into the representative aquifer is shown in Figure 6. The representative cost and range of costs presented in Figure 10 compare well with the DOE[23] study, in which the cost of storage for a 500 MW IGCC plant is quoted as being between $0.40 and $4.60 per tonne injected, and earlier studies[4] where the costs are on the order of $1 per tonne injected.

Figure 6 shows that the cost of storage decreases with increasing plant size, and decreases with increasing surface injection pressure. However, Figure 10 illustrates only the cost of storage: the increasing cost of transport with increasing surface injection pressure may offset decreases in storage cost to some degree. The cost per tonne of CO_2 stored shows increasing returns to scale, much like the transport cost. Combining the

representative result for the cost of transport with the result for the cost of aquifer storage presented here, the total cost per tonne of transport and storage is about $1.14 per tonne of CO_2 stored.

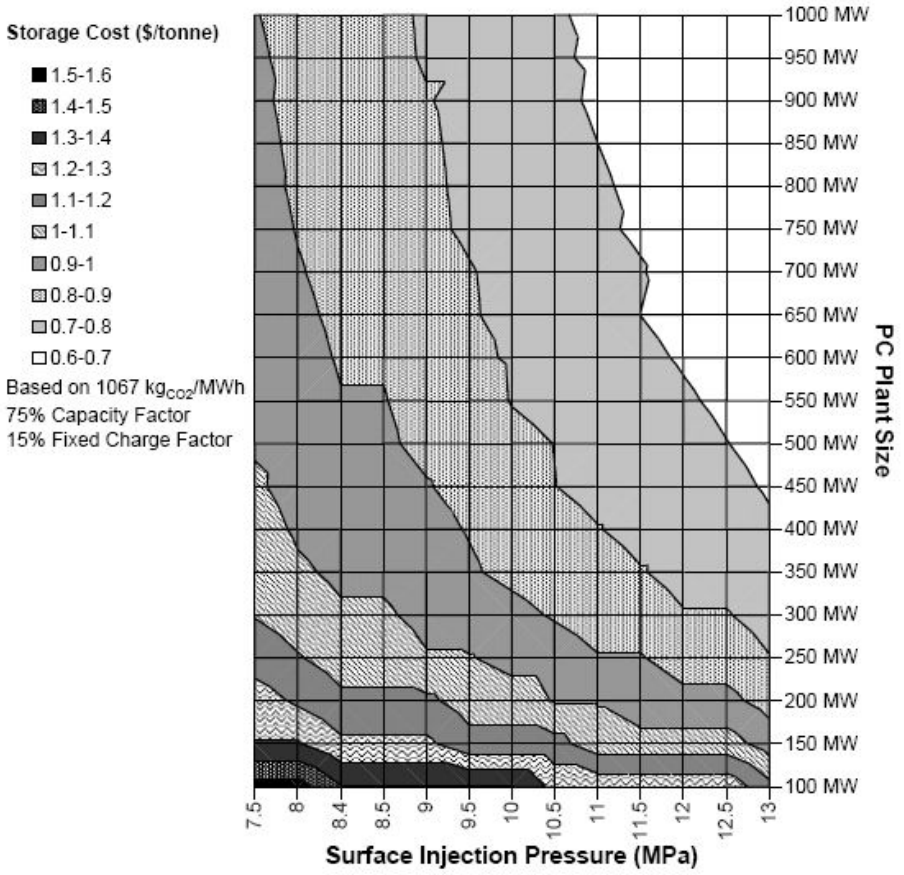

Figure 6. The cost of aquifer storage for varying capacities of coal fired power plants.

5.3. Sensitivity Study Results

The results of applying the probability distributions in Tables 3 and 4 to the transport and storage models, respectively, are shown by the cumulative distribution functions shown in Figure 7. In Figure 7, the storage cost shows much greater variability than the transport cost given the uncertainty in the input parameters. Table 5 summarizes the results of the sensitivity analysis for transport, storage, and the total of the two costs.

Table 5. Summary statistics for the transport, storage, and total costs calculated in the sensitivity analysis.

Statistic	Transport Cost ($/tonne)	Storage Cost ($/tonne)	Total Cost ($/tonne)
Mean	0.55	3.74	4.29
Median	0.44	1.44	1.94
Standard Deviation	0.35	5.49	5.56
95% Percentile	1.22	14.01	14.59
5% Percentile	0.21	0.44	0.78
Minimum	0.12	0.32	0.60
Maximum	2.03	31.30	32.40

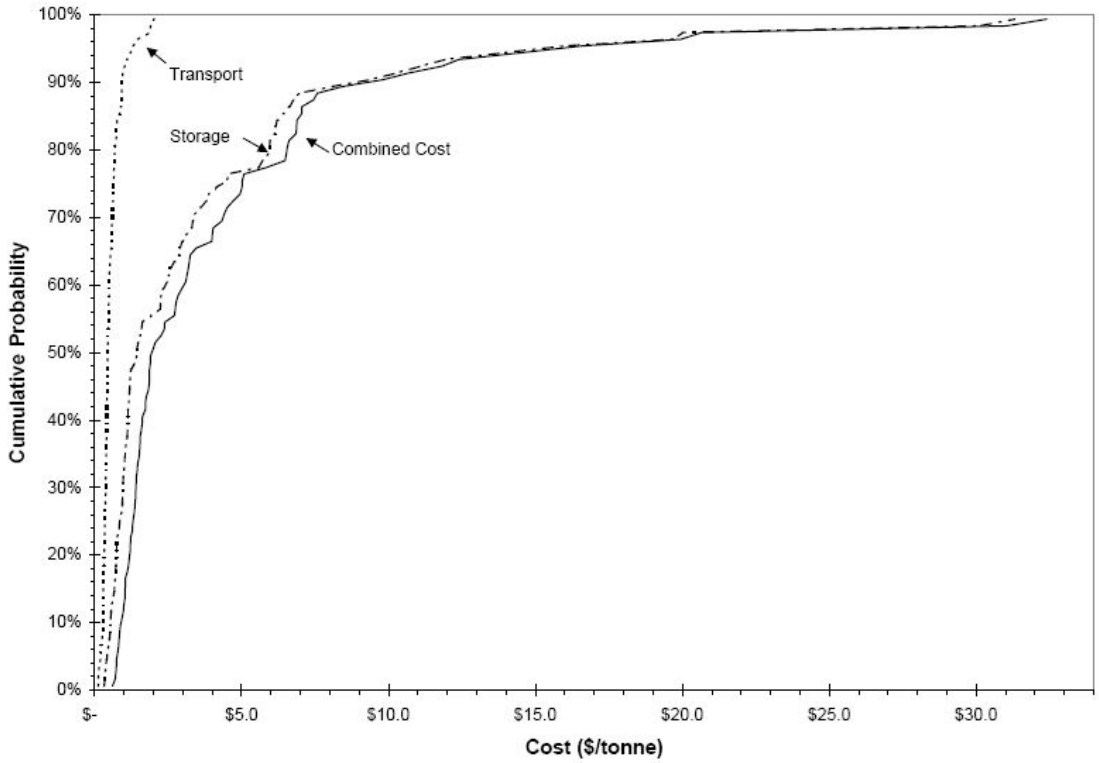

Figure 7. The cumulative probability distributions resulting from the Monte Carlo sensitivity analysis.

However, the degree to which the uncertainty in an individual input parameter contributes to the output is not clear from these results. Knowing which input parameters contribute most to the variability of the cost suggests where the greatest reduction in the cost estimate variability can be gained through a reduction in input uncertainty. In order to assess the relative contribution of uncertainty and variability to the cost calculated by the transport and storage models and, in turn, the total cost of transport and storage, Spearman rank-order correlation coefficients were calculated. The rank-order correlation coefficients are shown in Figure 8.

The dotted horizontal lines above and below the abscissa in Figure 8 indicate the 95% two-tailed confidence interval for the calculated rank-order correlation coefficients. Thus, in this scenario the correlation between the cost of transport, storage, or the total cost is not statistically significant for the following parameters: annual pipeline O&M, reservoir depth, reservoir thickness, monitoring and verification cost, and site screening and evaluation cost. Of the significant correlations, the variability in the reservoir permeability has the largest effect on the variability of both the cost of storage and the total cost, while the uncertainty in the pipeline length has the largest effect on the variability of the cost of transport and a barely significant effect on the total cost. The capacity factor has a significant impact on all of the cost estimates.

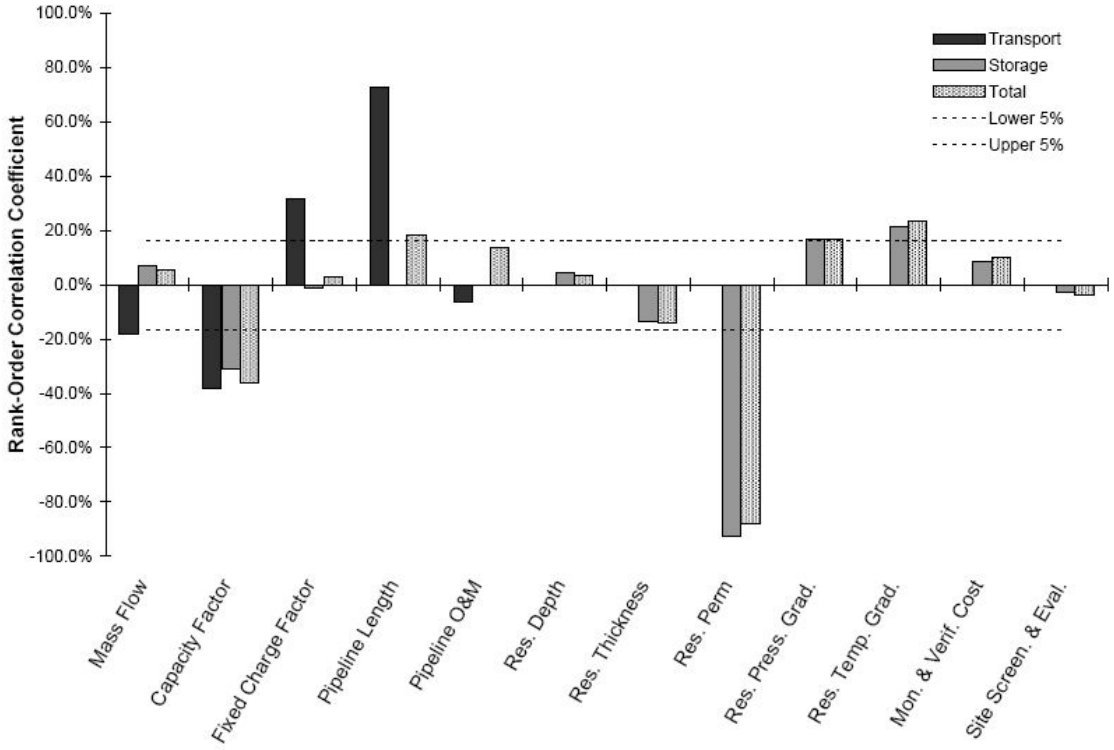

Figure 8. Rank-order correlation coefficients calculated between the transport cost (output) and the uncertain or variable input parameters.

The contribution of uncertainty and variability of the input parameters to the cost calculated by the models will be affected by the distributions used to define the uncertainty and variability of the inputs. Thus, for a different scenario, the relative contributions may change. For example, if the model was applied to a specific source-sink paring (e.g. a 500 MW PC plant 100km from a storage location), there would not be uncertainty in the pipeline length and CO_2 mass flow rate and the correlation coefficients of the remaining uncertain and variable parameters would likely increase. Moreover, the costs of transport and storage presented above does not necessarily reflect an estimate of the absolute cost of transport and storage for a power plant located in the Wabamun

Lake study area. For example, another formation for storage could be used that had a more favorable permeability that was located closer (or farther) from the power plant.

5.4. Policy Implications

Based on the results of the scenario presented above, the median cost of transport and storage ($1.44 per tonne) is less than 10% of the cost of capture, which are around $30 to $40 per tonne of CO_2 captured[43]. However, there is great variability in the cost that is mainly attributable to the distance between the point of capture and storage, the geological parameters of the aquifer, and the capacity factor. The effects of variability of these parameters on the total cost is significant and not considered in most papers on transport and storage cost, or in the papers that cite "typical" transport and storage costs[4,10,22,23,43]. While it is difficult to generalize these results, it is nonetheless safe to hypothesize that there would be a few cases in which the cost of transport and storage would be a large part (i.e. >50%) of the total storage cost. Thus, policies encouraging CCS must take into account that it will not be economically feasible in many cases.

Given that, in most cases, the cost of transport and storage is a small part of the overall storage cost, it is likely that cost of transport and storage will not be a limiting factor in its implementation at the global scale. However, there are other issues that may pose a problem such as regulatory concerns surrounding safety and long-term security of storage[44-46] and public perception of the technology[47]. These issues have yet to be adequately addressed, although they are being actively studied[48].

6. Conclusion

Storage of CO_2 can be accomplished by transporting CO_2 from the site of capture via pipeline, and injecting it into deep saline aquifers. The CO_2 must be transported at high pressures for efficiency, and injected into the saline aquifer at pressures greater than are present in the formation. For carefully selected and well characterized aquifers, it is expected to remain in the subsurface for centuries if not permanently. Engineering-economic models of these processes have been developed based on fundamentals of fluid flow in pipes and porous media, and historic costs from the petroleum industry. Applying the models to a scenario involving storage of CO_2 captured from a 500 MW coal fired power plant in the vicinity of Wabamun Lake in central Alberta, Canada with in a distribution of costs. The median cost for CO_2 transport is $0.44 per tonne, for storage is $1.44 per tonne, and the combined median cost of transport and storage is $1.94 per tonne CO_2 stored. The cost of CO_2 storage is more variable than that of CO_2 transport, and the total cost varies from a 5^{th} percentile of $0.78 per tonne to a 95^{th} percentile $14.59 per tonne. Based on these results, the median cost of transport and storage is a small part of the total cost of CO_2 storage, but there will be cases in which the cost of transport and storage are large.

The uncertainty analysis has shown that the parameters which have the most impact on the variability of the transport cost are the length of the CO_2 pipeline and the amount of CO_2 to be transported, while the cost of injecting CO_2 is highly dependent on the permeability of the host formation. The cost of CO_2 transport increases with distance and decreases with pipeline capacity, resulting in economies of scale that are reached at high design capacities. The cost

of CO_2 storage increases exponentially as permeability decreases and the cost of both transport and storage are decreased with increasing capacity factors. The significant dependence of transport and storage cost on reservoir parameters, transport distances, and capacity factors suggests that future studies should carefully consider these factors when citing general cost estimates.

7. References

[1] Hoffert MI, Calderia K, Jain AK, et al. Energy implications of future stabilization of atmospheric CO2 contnent. Nature 1998; 395: 881-884.

[2] Hoffert MI, Calderia K, Benford G, et al. Advanced Technology Paths to Global Climate Stability: Energy for a Greenhouse Planet. Science 2002; 298: 981-987.

[3] Bachu S. Screening and ranking of sedimentary basins for sequestration of CO2 in geological media in response to climate change. Environ. Geol. 2003; 44: 277-289.

[4] Hendriks CF. Carbon Dioxide Removal from Coal Fired Power Plants. Dordecht (NL): Kluwer Academic Publishers; 1994. 250 p.

[5] Parsons Infrastructure & Technology Group. Evaluation of Fossil Fuel Power Plants with CO_2 Recovery [Final Report to USDOE]. Morgantown, WV: National Energy Technology Laboratory; 2002. 134 p.

[6] White CM, Strazisar BR, Granite EJ, Hoffman JS, Pennline HW. Separation and Capture of CO2 from Large Stationary Sources and Sequestration in Geological Formations-Coalbeds and Deep Saline Aquifers. J. Air & Waste Manage. Assoc. 2003; 53: 645-715.

[7] Rao AB, Rubin ES. A Technical, Economic, and Environmental Assessment of Amine-Based CO2 Capture Technology for Power Plant Greenhouse Gas Control. Environ. Sci. Technol. 2002; 36: 4467-4475

[8] Energy Information Administration (US) [EIA]. Emissions of Greenhouse Gases in the United States 2003 [report on Internet]. Washington, DC: EIA; 2004 December [Cited 2005 April 13] . 124 p. Available from: ftp://ftp.eia.doe.gov/pub/oiaf /1605/cdrom/pdf/ggrpt/ 057303.pdf

[9] Svensson R, Odenberger M, Johnsson F, Stromberg L. Transportation systems for CO2 – application to carbon capture and storage. Energy. Convers. Manage. 2004; 45: 2243-2353.

[10] Skovholt O. CO2 Transportation System. Energy Convers. Manage. 1993; 34: 1095-1103.

[11] Bachu S. Sequestration of CO_2 in geological media in response to climate change: road map for site selection using the transform of the geological space into the CO_2 phase space. Energy Convers. Manage. 2002; 43: 87-102.

[12] Hendriks CA, Blok K. Underground Storage of Carbon Dioxide. Energy Convers. Manage. 1995; 36: 539-542

[13] Holloway S. Storage of Fossil Fuel-Derived Carbon Dioxide Beneath the Surface of the Earth. Annu. Rev. Energy Environ. 2001; 26: 145-166.

[14] Koide H, Tazaki Y, Noguchi Y, Nakayama S, Iijima M, Ito K, Shindo Y. Subterranean Containment and Long-Term Storage of Carbon Dioxide in Unused Aquifers and in Depleted Natural Gas Reservoirs. Energy Convers. Manage. 1992; 33: 619-626

[15] Bachu S, Gunter WD, Perkins EH. Aquifer disposal of CO_2: hydrodynamic and mineral trapping. Energy Convers. Manage. 1994; 35: 269-279.

[16] Stevens S, Kuuskraa VA, Gale J. Sequestration of CO2 in Depleted Oil & Gas Fields: Global Capacity, Costs, and Barriers. Proceedings of the Fifth International Conference on Greenhouse Gas Control Technologies; Cairns, Australia: 2000 Aug. 13-16: CSIRO Publishing; 2001. 1348 p.

[17] Shaw J, Bachu S. Screening, Evaluation, and Ranking of Oil Reservoirs Suitable for CO_2-Flood EOR and Carbon Dioxide Sequestration. J. Can. Pet. Technol. 2002; 41(9): 51-61

[18] Gunter WD, Wong S, Cheel DB, Sjostrom G. Large CO2 Sinks: Their Role in the Mitigation of Greenhouse Gases from an International (Canadian) and Provincial (Alberta) Perspective. Appl. Energy. 1988; 61: 209-227

[19] Stevens SH, Kuuskra VA, Spector D, Reimer P. CO_2 Sequestration in Deep Coal Seams: Pilot Results and Worldwide Potential. Proceedings of the Fourth International Conference on Greenhouse Gas Control Technologies; Interlaken, Switzerland: 1998 Aug. 30-Sept. 3: Elsevier; 1999.

[20] Bachu S, Adams JJ. Sequestration of CO2 in geological media in response to climate change: capacity of deep saline aquifers to sequester CO2 in solution. Energy Convers. Manage, 2003; 44: 3151-3175.

[21] Gale J, Davison J. Transmission of CO_2- safety and economic considerations. Energy. 2004; 29: 1319-1328.

[22] Smith L, Gupta N, Sass B, Bubenik T. Carbon Dioxide Sequestration in Saline Formations- Engineering and Economic Assessment [Final Report to USDOE]. Columbus, OH: Battelle Memorial Institute; 2001. 92 p.

[23] Bock B, Rhudy R, Herzog H, et al. Economic Evaluation of CO2 Storage and Sink Enhancement Options [Final Report to USDOE]. Muscle Shoals, TN: TVA Public Power Institute; 2003. 500 p.

[24] Kinder Morgan CO_2 Company. Dallas, TX: Kinder Morgan, Inc; c2002 [Cited 2004 Dec 23]. Available from: http://www.kne.com/business/co2/transport.cfm#co2_pipelines

[25] International Energy Agency [IEA] Greenhouse Gas R&D Programme. Pipeline Transmission of CO_2 and Energy Transmission Study- Report. Report Number PH4/6. Cheltenham, UK: IEA; 2002 Feb. 61 p.

[26] Zigrang DJ, Sylvester ND. Explicit Approximations to the Solution of Colebrook's Friction Factor Equation. AIChE Journal 1982; 28: 514-515.

[27] Torp TA, Gale J. Demonstrating storage of CO_2 in geological reservoirs: The Sleipner and SACS projects. Energy. 2004; 29: 1361-1369.

[28] Korbol R, Kaddour A. Sleipner Vest CO_2 Disposal- Injection of Removed CO_2 into the Utsira Formation. Energy Convers. Manage. 1995; 36: 509-512.

[29] Torp TA, Brown KR. CO_2 Underground Storage Costs as Experienced at Sleipner and Weyburn. In: Proceedings of the Seventh International Conference on Greenhouse Gas Control Technologies; Vancouver, Canada: 2004 Sept. 5-9: *In Press*.

[30] Bachu S, Gunter WD. Overview of Acid-Gas Injection Operations in Western Canada. In: Proceedings of the Seventh International Conference on Greenhouse Gas Control Technologies; Vancouver, Canada: 2004 Sept. 5-9: *In Press*.

[31] Bachu S, Haug K. In-Situ Characteristics of Acid-Gas Injection Operations in the Alberta Basin, Western Canada: Demonstration of Geological CO_2 Storage. In: Benson, SM. The CO_2 Capture and Storage Project (CCP) for Carbon Dioxide Storage in Deep Geologic Formations for Climate Change Mitigation. 2 Volumes. London, UK: Elsevier; 2005. Vol. 2: *In Press.*

[32] Law DHS, Bachu S. Hydrogeological and Numerical Analysis of CO2 Disposal in Deep Aquifers in the Alberta Sedimentary Basin. Energy Convers. Manage. 1996; 37: 1167-1174.

[33] van der Meer LGH. Investigations regarding the storage of carbon dioxide in aquifers in The Netherlands. Energy Convers. Manage. 1992; 33: 611-618.

[34] Energy Information Administration (US) [EIA]. Costs and Indices for Domestic Oil and Gas Field Equipment and Production Operations [report on Internet]. Washington, DC: EIA; 2004 April [Cited 2004 September 22]. Available from: http://www.eia.doe.gov/pub/oil_gas/

[35] American Petroleum Institute [API]. 1998 Joint Association Survey on Drilling Costs [subscription based report on Internet]. Washington, DC: API; 2004 April [Cited 2004 September 22]. Available from: http://www.api.org/axs-api/products/joint.htm

[36] Gunter WD, Bachu S, Perkins EH, et al. Aquifer Disposal of CO_2-Rich Gases in the Vicinity of the Sundance and Genesee Power Plants, Phase I: Injectivity, chemical reactions and proof of concept. Edmonton (AB): Alberta Research Council [ARC]; March 1993. 116 p. Available from: ARC, Edmonton, AB; Open File Report 1994-16

[37] Our Plants @ A Glance. Calgary, AB: TransAlta Corporation; c2004 [Cited 2005 Jan 1]. Available from:

http://www.transalta.com/website2001/tawebsite.nsf/AllDoc/2015CE3BDE2D8A4F872569AE007079B5?OpenDocument

[38] Gunter WD, Bachu S, Law DHS, et al. Technical and Economic Feasibility of CO_2 Disposal in Aquifers within the Alberta Sedimentary Basin, Canada. Energy. Convers. Manage. 1996; 37: 1135-1142.

[39] US Environmental Protection Agency- Clean Energy [Internet]. Washington: EPA; c2004 [Cited 2004 May 23]. Available from: http://www.epa.gov/cleanenergy/egrid/index.htm

[40] Meyer LR, Hoversten GM, Gasperikova E. Sensitivity and Cost of Monitoring Geologic Sequestration Using Geophysics. In: Proceedings of the Sixth International Conference on Greenhouse Gas Control Technologies; Kyoto, Japan: 2002 Oct. 1-4: London, UK; 2003. 1940 p.

[41] Benson SM, Cook P. Status and current issues in geologic storage of carbon dioxide. In: Proceedings of the Seventh International Conference on Greenhouse Gas Control Technologies; Vancouver, Canada: 2004 Sept. 5-9: *In Press*.

[42] Gunter WD, Bachu S, Perkins EH, et al. Central Alberta: CO_2 Disposal into Alberta Basin Aquifers, Phase II: Hydrogeological and Mineralogical Characterization of Mannville Group Strata in the Lake Wabamun Area. Edmonton (AB): Alberta Research Council [ARC]; March 1993. 121 p. Available from: ARC, Edmonton, AB; Open File Report 1994-17

[43] Rubin ES, Rao AB, Chao C. Comparitive Assessments of Fossil Fuel Power Plants with CO_2 Capture and Storage. In: Proceedings of the Seventh International Conference on Greenhouse Gas Control Technologies; Vancouver, Canada: 2004 Sept. 5-9: *In Press*.

[44] Bruant RG, Celia MA, Guswa AJ, Peters CA. Safe Storage of CO_2 in Deep Saline Aquifers. Enivrion. Sci. Technol. 2002; 36: 240A-245A

[45] Wilson EJ, Johnson TJ, Keith DW. Regulating the Ultimate Sink: Managing the Risks of Geological CO_2 Storage. Environ. Sci. Technol. 2003; 37: 3746-3483.

[46] Wilson EJ, Keith DW, Wilson M. Considerations for a Regulatory Framework for Large-Scale Geological Sequestration of Carbon Dioxide: A North-American Perspective. In: Proceedings of the Seventh International Conference on Greenhouse Gas Control Technologies; Vancouver, Canada: 2004 Sept. 5-9: *In Press*.

[47] Palmgren C, Morgan MG, Bruine de Bruin W, Keith DW. Initial public perceptions of deep geological and oceanic disposal of CO_2. In: Proceedings of the Seventh International Conference on Greenhouse Gas Control Technologies; Vancouver, Canada: 2004 Sept. 5-9: *In Press*.

[48] Gale, J. Geological storage of CO_2: What do we know, where are the gaps and what more needs to be done? Energy. 2004; 29: 1329-1338.

A. Appendix: Nomenclature

Symbol	Variable	Units
Z_i	Height at location *i*	m
α_i	Kinetic energy conversion factor	-
$\overline{V}_i$	Average velocity at location *i*	m/s
η	Pump efficiency	-
w_s	Shaft (e.g., pump) work	kJ/kg
h_f	Head losses due to friction	kJ/kg
f_F	Fanning friction factor	-
ε	Pipe roughness	mm
Re	Reynolds number	-
p	Pressure	Pa
p_i	Pressure at location *i*	Pa
p_a	Far field pressure in aquifer	Pa
ρ_w	Density of formation water	kg/m^3
ρ_i	Density in segment *i*	kg/m^3
g	Acceleration due to gravity	m/s^2
g_c	Gravitational constant	-
f_F	Fanning friction factor	-
ΔL	Pipe segment length	m
D	Pipe inner diameter	m
D_1	Initial segment diameter	m
D_n	n^{th} segment diameter	m
N_S	Number of segments	-
N_B	Number of booster pumping stations	-
N_W	Number of wells	-
C_P	Cost of power	$/MWh
$\dot{m}$	Mass flow rate	kg/s
$\dot{m}_w$	Mass flow rate per well	kg/s/well
ε	Pipe roughness	mm
Re	Reynolds number	-
μ	Viscosity	Pa s
h	Aquifer thickness	m
k	Formation permeability	10^{-15} m^2
k_r	Relative permeability of CO_2 in the formation	-
k_h	Horizontal formation permeability	10^{-15} m^2
k_v	Vertical formation permeability	10^{-15} m^2
d	Well depth	m

B. Appendix: Transport and Storage Model Mechanics

B.1. Transport Model Energy Balance

For the purpose of determining the diameter of a pipeline segment the dense phase CO_2 is considered an incompressible fluid. Furthermore, the pipeline flow process and pumping processes are treated as isothermal. This is a reasonable assumption as long as the pressure of the CO_2 entering the pipeline is not considerably (i.e., approximately 5 MPa) greater than the outlet pressure of the pipeline. Under these conditions, assuming that the outlet pressure is at least 10.3 MPa, the density of the CO2 will decrease at most about 5% over the length of the pipeline.

The pipe diameter is calculated from an energy balance on the flowing CO_2. Equation 1 gives the energy balance for the flowing CO2 between the inlet of the pipeline, a, and the outlet of the pipeline, b, assuming turbulent, incompressible flow*.

$$\frac{p_a}{\rho}+\frac{gZ_a}{g_c}+\frac{\alpha_a\overline{V}_a^2}{2g_c}+\eta w_s=\frac{p_b}{\rho}+\frac{gZ_b}{g_c}+\frac{\alpha_b\overline{V}_b^2}{2g_c}+h_f \qquad (1)$$

In Equation 1: p is the pressure at a given location; ρ is the density of the fluid; Z is the height of the fluid at a given location; α is the kinetic energy correction factor for locations a and b; $\overline{V}$ is the average velocity at a given location, and; h_f is the head loss due to friction between the inlet and the outlet.

For highly turbulent flow the kinetic energy correction factors are approximately 1.0*, and we assume that no pump work is performed over a pipeline segment- the pump model will handle pump work. Allowing for these simplifications, we arrive at Equation 2:

$$p_a-p_b=\Delta p=\rho g_c h_f-\frac{g}{g_c}\left(Z_a-Z_b\right) \qquad (2)$$

The head loss due to skin friction is related to other flow parameters by Equation 3:

$$h_{fs}=4f_F\frac{\Delta L}{D}\frac{\overline{V}^2}{2g_c} \qquad (3)$$

where f_F is the Fanning friction factor, D is the pipe inner diameter, and ΔL is the segment length. Substituting Equation 3 into Equation 2, we arrive at Equation 4:

* McCabe WL, Smith JC, Harriott, P. Unit Operations of Chemical Engineering. 5th ed. New York: McGraw-Hill; 1993. 1130 p.

$$\Delta p = \frac{2\rho f_F \Delta L \overline{V}^2}{g_c D} - \frac{g\rho\Delta Z}{g_c} \qquad (4)$$

The velocity is a function of the pipe diameter, thus substituting for velocity and rearranging expression in terms of diameter, we arrive at Equation 5 (given as Equation 1 in the main text body):

$$D = \left[\frac{32 f_F \Delta L \dot{m}^2}{\pi^2 \Delta p \rho + g\pi^2 \rho^2 \Delta Z} \right]^{1/5} \qquad (5)$$

B.2. Transport Model Pumping Stations

Equation 6 results from simplifying the mechanical energy balance assuming incompressible and isothermal flow, and no elevation or velocity change within the pump:

$$P = \frac{\dot{Q}\Delta p}{\eta} \qquad (6)$$

where P is the required pump size, $\dot{Q}$ is the volumetric flow rate, and η is the pump efficiency, which accounts for all frictional losses.

B.3. Transport Model Solution Method

The basic input and output screen is shown in Figure 1. From this input screen all of the pipeline parameters can be modified, and the model output viewed.

Pipeline Transport Model: Model Summary

January 2, 2005

Model Inputs		Model Outputs	
Pipeline Parameters		**Initial Segment Parameters**	
CO_2 Mass Flow [t yr^{-1}]	4.67E+06	$\Delta P/\Delta L$ [Pa m^{-1}]	116.33
Plant Capacity Factor [%]	75%	Average CO_2 Density [kg m^{-3}]	957.57
Inlet Temperature [°C]	5.6	Average CO_2 Viscosity [μPa s^{-1}]	108.16
Inlet Pressure [MPa]	13.79	Pipe Diameter [in]	11.5
Outlet Pressure [MPa]	10.3	Reynolds Number	5974972
Total Pipeline Legnth [km]	30	Pipe Segments	1
Pipline Elevation Change [m]	0		
Roughness [mm]	0.0457	**Pumping Parameters**	
		Length Between Stations [km]	-
Pumping Station Parameters		Pump Size [kW]	720
Number of Booster Stations	0	Annual Power Requirement [MWh]	4733
Compression Ratio	1.34		
Efficiency [%]	75%	**General Segment Parameters**	
		$\Delta P/\Delta L$ [Pa m^{-1}]	116.33
Economic Parameters		Average CO_2 Density [kg m^{-3}]	957.57
Annual O&M [$ km^{-1} y^{-1}]	$ 3,100	Average CO_2 Viscosity [μPa s^{-1}]	108.16
Annual Pump O&M [$ y^{-1} $pump^{-1}$]	1.5%	Pipe Diameter [in]	11.5
COE [$ MWh^{-1}]	$ 40.00	Reynolds Number	5974972
Capital Recovery Factor [%]	15%	Pipe Segments	0
		Economic Parameters	
		Total Capital Cost [$]	$ 7,255,705
		Annualized Capital Cost [$ y^{-1}]	$ 1,088,356
		Total O&M [$ y^{-1}]	$ 93,000
		Total Energy Cost [$ y^{-1}]	$ -
		Total Annual Cost [$]	$ 1,181,356
		Total Cost [$ t^{-1}]	$ 0.34

Click the base case button to the right to reset the model inputs to the base case values

Base Case

Figure 1. The summary screen for the transport model, showing the pipeline parameters

In order to accommodate the booster stations, the pipeline is broken up into segments, which are equal in length. The segment length, ΔL, and number, N_S, of the pipe segments is determined by the number of booster stations specified by the user, N_B, and the total pipeline length, L. The number of pipe segments is one greater than the number of booster stations and the segment length is the total length divided by the number of segments For example, for a 75 km pipeline if there are 2 booster pumping stations specified there are then 3-25 km long pipe segments. For the initial segment, the inlet pressure and outlet pressure are given by the Inlet Pressure and Outlet Pressure fields in the model input. For latter segments, the outlet pressure is fixed at the value in the Outlet Pressure field while the inlet pressure is determined by the pump compression ratio. Figure 2 shows the steps in the calculation of the pipeline diameter, and the overall algorithm.

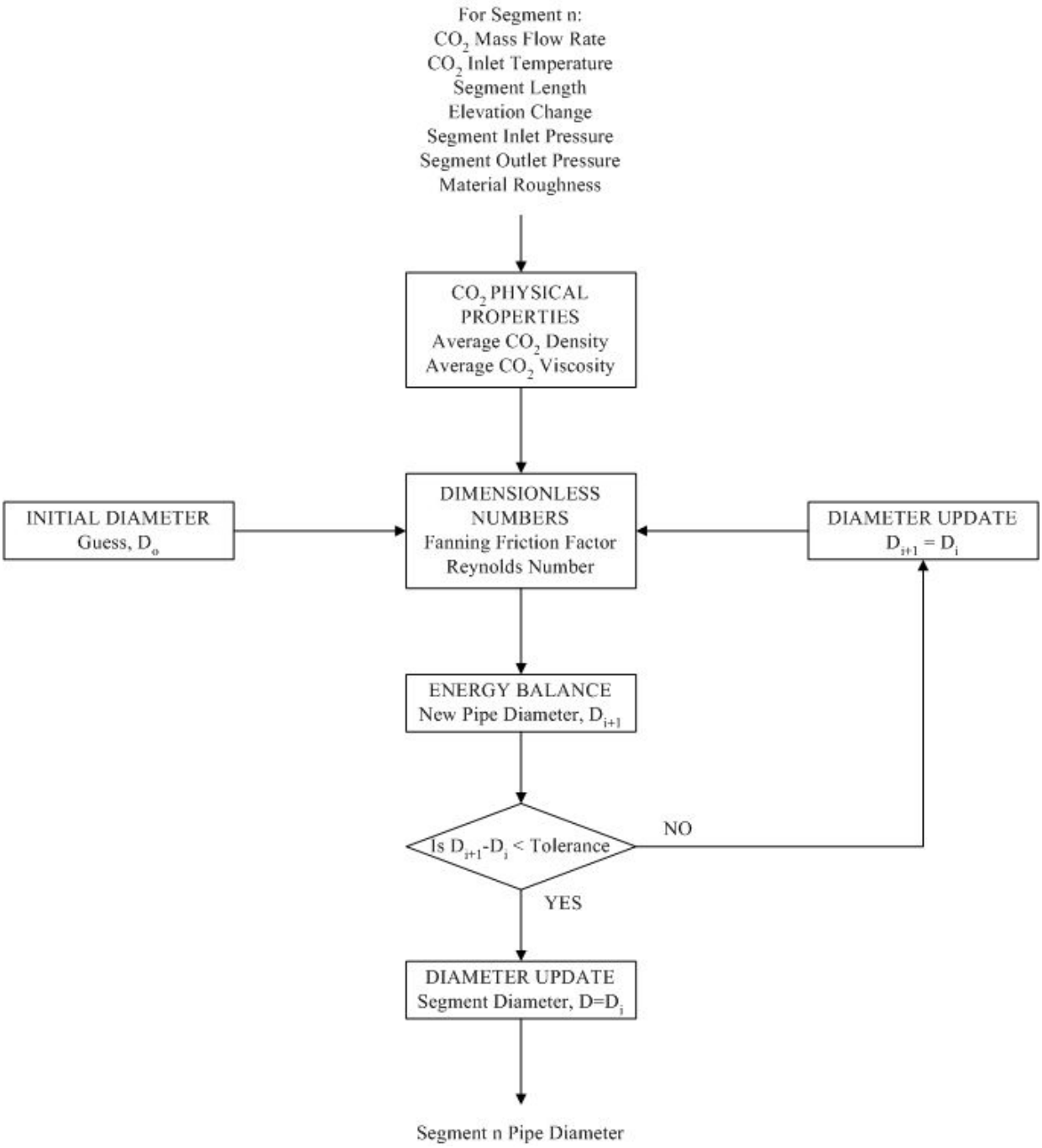

Figure 2. Flowchart showing the steps involved in the calculation of the pipeline diameter.

B.4. Injection Well Illustration

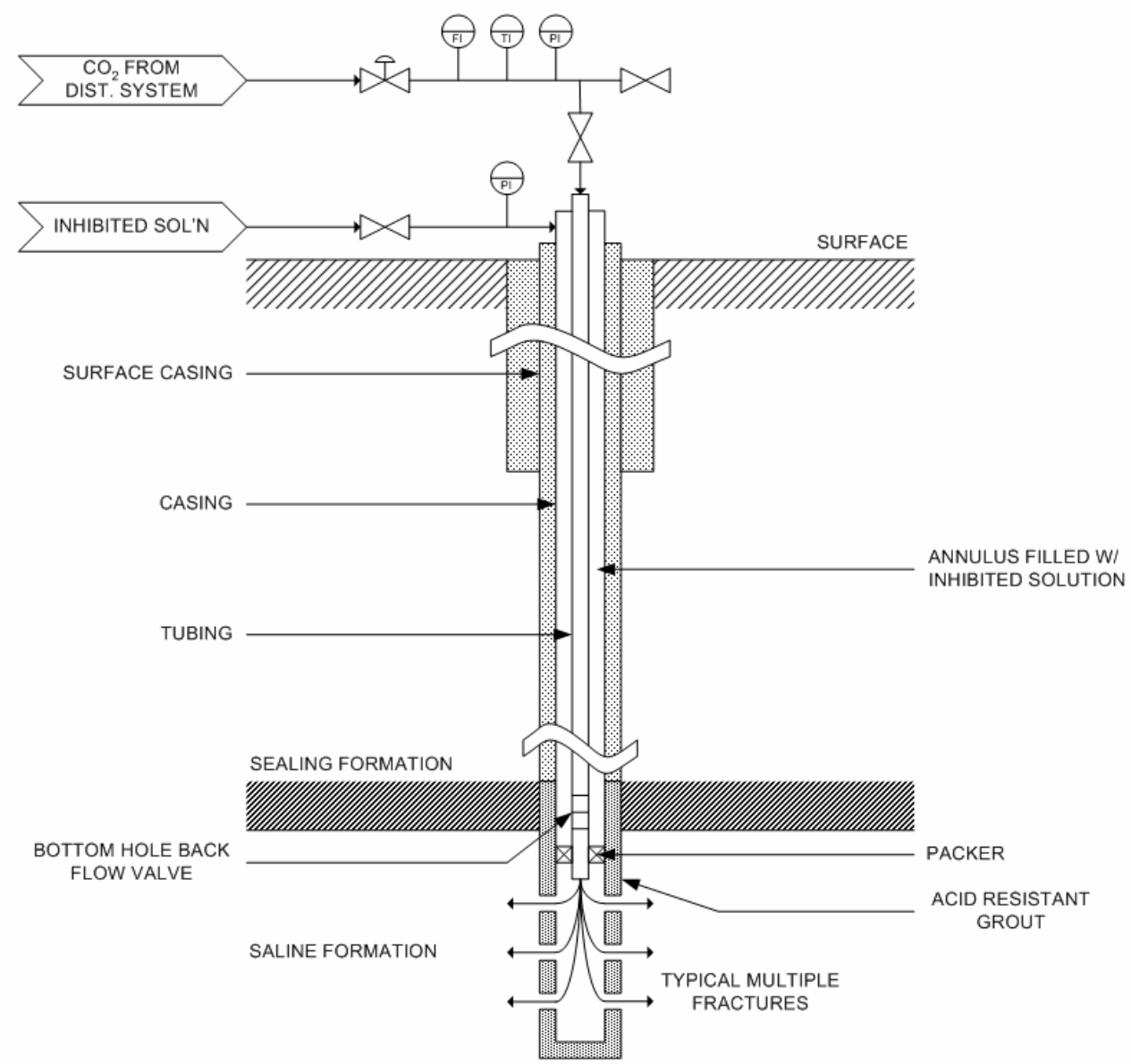

Figure 3. Illustration of the parts of a typical CO_2 injection well.

B.5. Bottom Hole Injection Pressure Model

The BHIP is calculated assuming that there is no heat transfer between the flowing surrounding formations to the CO_2 (i.e. adiabatic flow), and by treating flow over the entire length of the well as compressible, but flow over short intervals (i.e., ~10 m) as incompressible. Following these assumptions, the injection well is divided into small intervals and the physical properties of the CO_2, assumed constant over the length of the interval, are calculated at temperature and pressure at the top of the interval. Using these properties, the pressure drop due to friction losses assuming turbulent flow is calculated for the interval and subtracted from the pressure increase due to gravity head over the

interval. The temperature at the bottom of the interval is then calculated based on the enthalpy change over the interval and, with the calculated pressure, used for the calculations in interval below.

Energy balances on the flowing CO_2 give the pressure change and the enthalpy change over the calculation intervals in the injection well. Equation 7 shows the mechanical energy balance, which neglects the change in kinetic energy (i.e., velocity) of the CO_2 over the discretized interval. Equation 8 shows the enthalpy balance used for the temperature calculation.

$$p_j - p_{j+1} = \Delta p = 32 f_F \frac{\Delta L \dot{m}^2}{\pi^2 D^5 \rho_j} - g \rho_j \Delta L \qquad (7)$$

$$h_j - h_{j+1} = \Delta h = g \Delta L \qquad (8)$$

In Equation 7: p_j represents pressure at the top of segment j; f_F is the fanning friction factor; ΔL is the discretized segment length; $\dot{m}$ is the mass flow rate in the injection well; D is the well diameter; ρ_j is the density in segment j, and; g is the gravitational constant. Pressure drop due to skin friction between the flowing CO_2 and the pipe wall is given by the first term on the far right hand side of Equation 7, while the second term on the right is the pressure increase due to gravitational head. In Equation 8, h_j represents specific enthalpy at the top of segment j, and g represents acceleration due to gravity.

B.6. Injection Model Solution Method

The root of Equation 9 (also given as Equation 10 in the main text) occurs when the number of injection wells is appropriate for a given geology and injection rate. The approach to finding the root of the resulting function uses a combination of bracketing and Ridders' Method, as illustrated in Figure 3.

$$E(N_w) = \frac{\dot{m}}{N_w} - 0.000538 \frac{\rho (k_h k_v)^{0.5} h (p_i - p_a)}{\mu \ln\left(\frac{r_e}{r_w}\right)} \qquad (9)$$

The well number algorithm begins by calculating the value of the error function $E(N_w)$, Equation 9, for the initial well number $N_{w,o}$. Then the well number is incremented, and the value of the error function is calculated at $N_{w,1}$. If the product of the $E(N_w)$ calculated at $N_{w,0}$ and $N_{w,1}$ is less than zero the root of the function is located on the interval between $N_{w,0}$ and $N_{w,1}$. If the root is not located on the initial interval, the process continues until the root is located on an interval. In the figure, the root is located between $N_{w,3}$ and $N_{w,4}$. Once interval containing the root is located, then the value of the root is found by the Ridders' method.

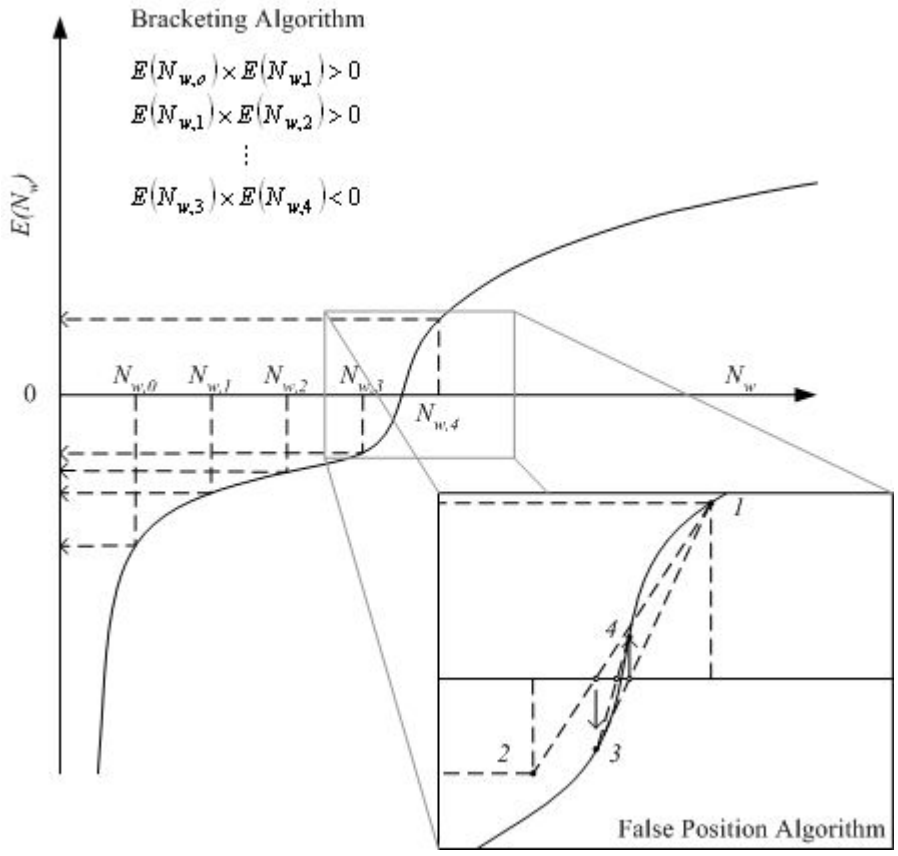

Figure 4. Figure showing the general shape of E(Nw) and the bracketing and false position routine.

Ridders' Method is a specific implementation of a false position method for finding the root of a function. In false position methods, the prior estimate of the root is retained when the function value has opposite sign from the function value at the current best estimate of the root. The false position method, illustrated in the enlarged part of Figure 3, begins by using linear interpolation to find the root of the linear approximation between points *1* and *2*. The value of *E(3)* is negative, and opposite in sign of *E(1)*, thus point *2* is discarded and point *1* is retained. The next linear interpolation between points *1* and *3* results in point *4*; the value of *E(4)* is opposite in sign of *E(3)*, thus point *3* is retained and *1* is discarded. This iterative process repeats until the length of the interval containing the root is less than 10^6. The general false position method illustrated in Figure 3 and Ridders' Method differ because Ridders' Method uses quadratic rather than linear interpolation[†].

Figure 4 illustrates the order of execution of the algorithm described above in the text and graphically in Figure 3. The bottom hole pressure calculation, injectivity-mobility correlation and the rate error function are all calculated by functions programmed in Visual Basic. Figure 5 is a screen shot of the basic input screen. From this input screen

[†] Press WH, Teukolsky SA, Vetterling WT, Flannery BP. Numerical Recipes in C: The Art of Scientific Computing. 2nd ed. Cambridge (UK): Cambridge University Press; 1992. 965 p.

all of the main geological, engineering, and economic parameters can be modified, and the model output viewed.

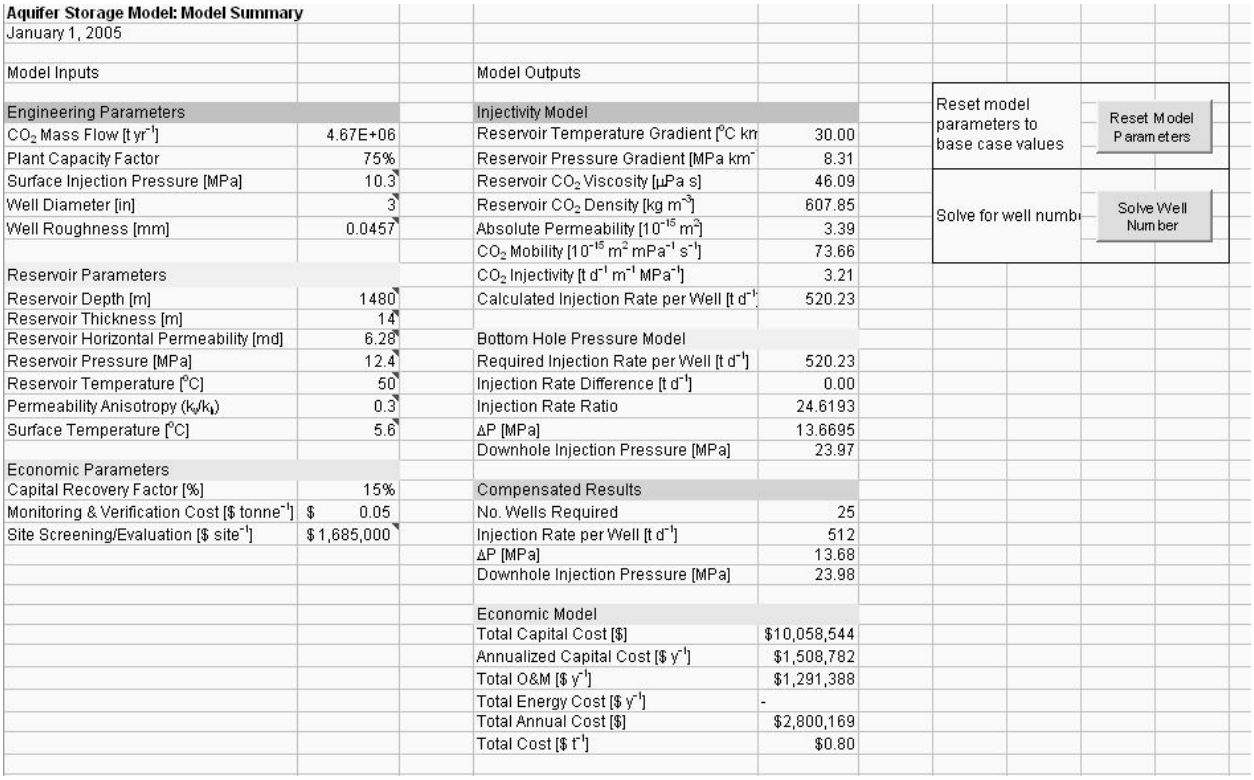

Aquifer Storage Model: Model Summary				
January 1, 2005				
Model Inputs		Model Outputs		
Engineering Parameters		Injectivity Model		
CO_2 Mass Flow [t yr^{-1}]	4.67E+06	Reservoir Temperature Gradient [°C km	30.00	
Plant Capacity Factor	75%	Reservoir Pressure Gradient [MPa km	8.31	
Surface Injection Pressure [MPa]	10.3	Reservoir CO_2 Viscosity [µPa s]	46.09	
Well Diameter [in]	3	Reservoir CO_2 Density [kg m^{-3}]	607.85	
Well Roughness [mm]	0.0457	Absolute Permeability [10^{-15} m^2]	3.39	
		CO_2 Mobility [10^{-15} m^2 mPa^{-1} s^{-1}]	73.66	
Reservoir Parameters		CO_2 Injectivity [t d^{-1} m^{-1} MPa^{-1}]	3.21	
Reservoir Depth [m]	1480	Calculated Injection Rate per Well [t d^{-1}	520.23	
Reservoir Thickness [m]	14			
Reservoir Horizontal Permeability [md]	6.28	Bottom Hole Pressure Model		
Reservoir Pressure [MPa]	12.4	Required Injection Rate per Well [t d^{-1}]	520.23	
Reservoir Temperature [°C]	50	Injection Rate Difference [t d^{-1}]	0.00	
Permeability Anisotropy (k_v/k_h)	0.3	Injection Rate Ratio	24.6193	
Surface Temperature [°C]	5.6	ΔP [MPa]	13.6695	
		Downhole Injection Pressure [MPa]	23.97	
Economic Parameters				
Capital Recovery Factor [%]	15%	Compensated Results		
Monitoring & Verification Cost [$ $tonne^{-1}$]	$ 0.05	No. Wells Required	25	
Site Screening/Evaluation [$ $site^{-1}$]	$ 1,685,000	Injection Rate per Well [t d^{-1}]	512	
		ΔP [MPa]	13.68	
		Downhole Injection Pressure [MPa]	23.98	
		Economic Model		
		Total Capital Cost [$]	$10,058,544	
		Annualized Capital Cost [$ y^{-1}]	$1,508,782	
		Total O&M [$ y^{-1}]	$1,291,388	
		Total Energy Cost [$ y^{-1}]	-	
		Total Annual Cost [$]	$2,800,169	
		Total Cost [$ t^{-1}]	$0.80	

Figure 5. The summary screen for the storage model, showing the pipeline parameters.

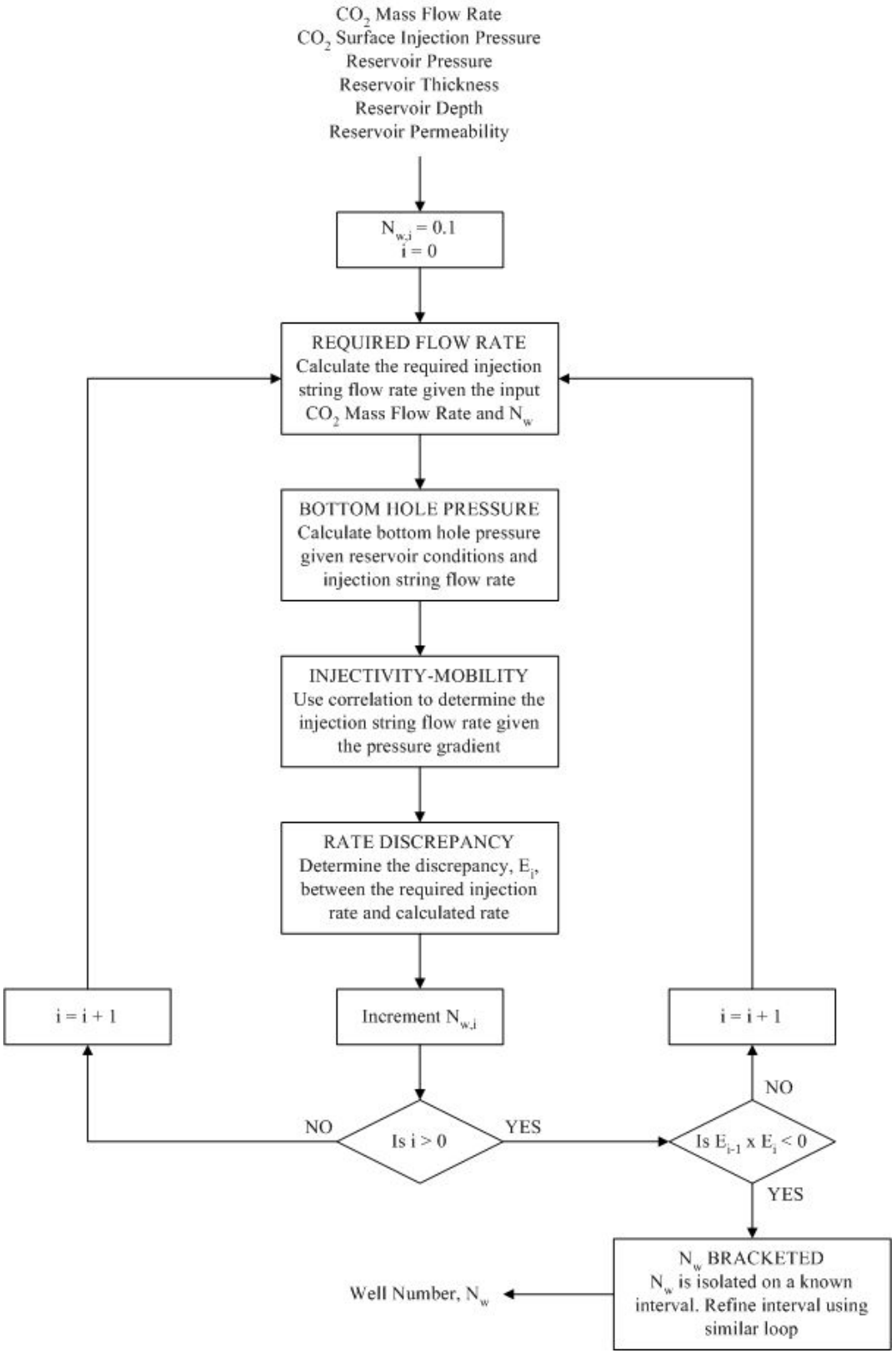

Figure 6. The order of execution of the algorithm used to solve for the number of wells required in the storage model.